

Observation of Pure Nuclear Diffraction from a Fe/Cr Antiferromagnetic Multilayer

T. S. Toellner, W. Sturhahn, R. Röhlberger, E. E. Alp, C. H. Sowers, and E. E. Fullerton

Argonne National Laboratory, 9700 South Cass Avenue, Argonne, Illinois 60439

(Received 28 October 1994)

We report the observation of nuclear resonant diffraction of synchrotron radiation from a $^{57}\text{Fe}/\text{Cr}$ multilayer. The multilayer consists of 25 $^{57}\text{Fe}(17 \text{ \AA})/\text{Cr}(10 \text{ \AA})$ bilayers with the Cr layer thickness chosen so as to exhibit antiferromagnetic (AF) coupling of the ^{57}Fe layers. Because of the AF alignment of the layers, the magnetic periodicity of the multilayer is twice the electronic periodicity, resulting in a pure nuclear Bragg reflection that appears during nuclear resonant diffraction. The pure nuclear Bragg reflection presents a means of filtering synchrotron radiation to the level of 10^{-8} eV at the nuclear resonance energy of 14.4 keV.

PACS numbers: 76.80.+y, 75.70.Cn, 78.70.Ck

The discovery of oscillatory interlayer coupling in Fe/Cr superlattices [1,2] has stimulated considerable interest. Superlattices that possess antiferromagnetic (AF) coupling of the ferromagnetic layers demonstrate unique magnetic phenomena such as giant magnetoresistance [3] and allow superlattices to be designed that mimic the properties of two-sublattice antiferromagnets [4]. In this Letter, we present the results of nuclear resonant diffraction of 14.4 keV synchrotron radiation from an AF coupled $^{57}\text{Fe}/\text{Cr}$ superlattice. As a result of the magnetic ordering of the superlattice, we observe a pure nuclear reflection, an effect originally observed by diffraction from a two-sublattice antiferromagnetic crystal containing ^{57}Fe [5–8]. In addition, we show that the resonantly scattered radiation from the multilayer is sensitive to the hyperfine field distribution and hence may be used to probe the magnetic structure of thin films.

If an Fe/Cr superlattice is produced using ^{57}Fe , then the sample may be probed using the 14.4 keV nuclear resonance in ^{57}Fe . Using synchrotron radiation (SR) to excite this resonance in a Bragg scattering geometry and subsequently measuring the time distribution of the resonantly scattered radiation allows one to probe the hyperfine interactions within the superlattice. Such nuclear resonant diffraction has been performed on single crystals containing ^{57}Fe in order to probe the magnetic structure. In the case of nuclear resonant Bragg diffraction from single crystals, the long-range order of hyperfine interactions may give rise to pure nuclear Bragg reflections. Pure means that the structure factor for charge scattering vanishes, while that for resonant scattering does not. In general, pure nuclear Bragg reflections occur whenever the crystallographic symmetry group is not a subgroup of the symmetry group for the hyperfine interactions (on resonant nuclei). An antiferromagnetic alignment of magnetic sublattices will produce pure nuclear reflections for this reason. Pure nuclear reflections due to antiferromagnetic ordering of magnetic sublattices have been observed with single crystals of $^{57}\text{FeBO}_3$ and $^{57}\text{Fe}_2\text{O}_3$ using SR [5,6] and radioactive sources [7,8]. In addition, by

performing time-differential measurements in conjunction with nuclear resonant diffraction, one has the potential to gain both information on the local hyperfine interactions as well as information on the long-range order of these interactions [9]. Applying this technique in an analogous fashion to thin films containing ^{57}Fe , or other Mössbauer isotopes, would allow one to investigate the magnetic ordering within the layered system by probing the alignment of the magnetic hyperfine field.

Recently, a pure nuclear Bragg reflection has been produced in a synthesized multilayer with a ^{57}Fe isotopic unit cell that is double the charge unit cell ($^{57}\text{Fe}/\text{Sc}/^{56}\text{Fe}/\text{Sc}$) [10]. In the present Letter, we report the observation of a pure nuclear reflection due to *magnetic* ordering from a synthetic multilayer consisting of 17 \AA ^{57}Fe layers separated by 10 \AA Cr layers. The Cr layer thickness was chosen to produce antiferromagnetic coupling of the ^{57}Fe layers. This interlayer coupling results in a periodicity of magnetic hyperfine interactions that is twice the charge density periodicity. The resulting difference between the magnetic unit cell and the charge unit cell gives rise to a pure nuclear Bragg reflection.

The substrate/ $^{57}\text{Fe}(60 \text{ \AA})/[\text{Cr}(10 \text{ \AA})/^{57}\text{Fe}(17 \text{ \AA})]_{25}/\text{Cr}(20 \text{ \AA})$ superlattice was grown by dc magnetron sputtering. A smaller sapphire substrate was mounted adjacent to the main substrate for subsequent magnetic measurements. The ^{57}Fe was sputtered from a 3.8 cm diam natural Fe target on which a 95% enriched ^{57}Fe foil was spot welded to cover the region where the majority of the sputtering occurred. The Cr was sputtered from a 5 cm sputtering source with a 99.9% pure Cr target. The base pressure of the sputtering system was 1×10^{-7} Torr and the Ar sputtering pressure was 3.5 mTorr. The substrate-to-target distance was 8 cm, and deposition rates were kept constant at approximately $2 \text{ \AA}/\text{s}$. It has been previously found that sputtering under these growth conditions produces smooth layers with limited cumulative roughness for many materials [11]. The substrate was mounted on a computer-controlled sample holder, which passed the substrate sequentially over the Fe and

Cr sources. Because the sputtering sources are relatively small compared to the size of the substrate, the motion of the substrate was chosen to ensure thickness uniformity over the length of the substrate. Under the present growth conditions, it is expected that the thickness of the ^{57}Fe layers will be constant to better than 5% over the width (2.5 cm) of the substrate. This should result in negligible deviations of the ^{57}Fe layer thickness over the width of the incident synchrotron beam (1.0 cm).

Characterization of the hyperfine fields within the ^{57}Fe layers was performed using conversion electron Mössbauer spectroscopy (CEMS). A CEMS spectrum taken using a $^{57}\text{Co}(\text{Rh})$ radioactive source is shown in the inset of Fig. 1. A distribution of magnitudes of magnetic hyperfine fields (shown in Fig. 1) was needed to fit the spectrum. From the weighted set of Gaussian distributions used to fit the data, 42(8)% of the ^{57}Fe in the layers possess the magnetic hyperfine field of bulk α -Fe (33.3 T). The remainder of the ^{57}Fe possesses varying magnitudes of hyperfine fields. The percentages of five other hyperfine field strengths are 28% of ^{57}Fe at 30.7 T, 11% at 26 T, 5% at 22 T, 6% at 20 T, and 10% at 10 T. This result is in agreement with the CEMS studies on Fe/Cr films of Landes *et al.* [12]. The CEMS result also indicates minimal diffusion of ^{57}Fe into the Cr layers, with approximately 0.1% of ^{57}Fe having a magnetic hyperfine field less than 1.0 T. Magnetic measurements using a DC SQUID magnetometer on the superlattice grown on the sapphire substrate demonstrate that the ^{57}Fe layers are antiferromagnetically coupled with a saturation field greater than 1 T, as expected for a 10 Å Cr layer [1–4].

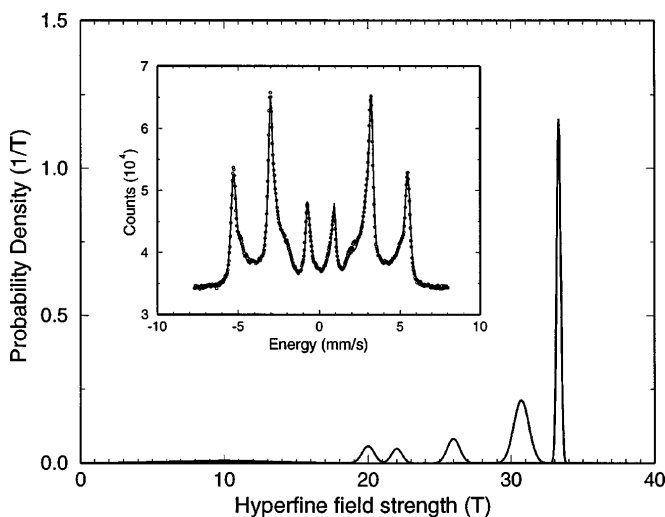


FIG. 1. The distribution of magnetic hyperfine fields within the $^{57}\text{Fe}/\text{Cr}$ multilayer used to produce the fit to the CEMS data (inset). Note that the CEMS data depend on the distribution of magnitudes and orientation of hyperfine fields, while nuclear resonant diffraction depends, in addition, on the location of those hyperfine fields.

To perform nuclear resonant diffraction from the multilayer, we used synchrotron radiation produced by a 24-pole wiggler on the F-2 beamline at Cornell's High Energy Synchrotron Source (CHESS). X rays produced by the wiggler were directed through an aperture and delivered to a water-cooled, double-crystal monochromator composed of Si(111) crystals to decrease the energy bandwidth to approximately 4 eV (FWHM) at the ^{57}Fe nuclear resonance energy of 14.413 keV. Because of the narrow resonance bandwidth ($\Gamma \sim 10^{-8}$ eV), the ratio of resonant flux to nonresonant flux is 10^{-9} . To reduce the nonresonant flux to a level that the detector can handle, we further monochromatized the beam using a high-resolution crystal monochromator of a nested design [13] to an energy bandwidth of 6 meV (FWHM) and with a vertical beam divergence of ≈ 20 μrad . From here, the 0.3 mm \times 10 mm horizontally polarized beam was vertically scattered from the $^{57}\text{Fe}/\text{Cr}$ multilayer. An external magnetic field of approximately 0.1 T was applied perpendicular to the scattering plane to eliminate magnetic domain formation in the film. After scattering from the sample, the radiation was collected by an avalanche photodiode (APD) detector that has a time resolution of ≤ 1 ns and an efficiency of 12% at 14.413 keV. Because of the presence of ^{57}Fe the scattered radiation from the multilayer contains both a prompt nonresonant component and a delayed (by a time on the order of $\tau \approx \hbar/\Gamma$) resonant component. As a result of the time delay, the resonant radiation can

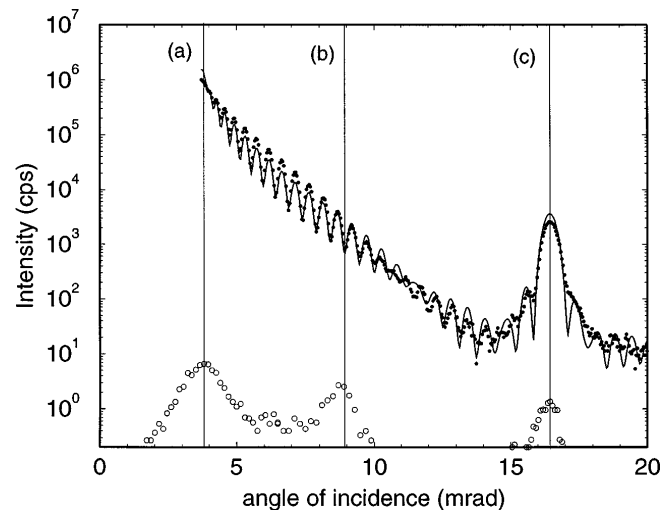


FIG. 2. The electronic reflectivity of the $^{57}\text{Fe}/\text{Cr}$ multilayer (filled circles) with a fit (solid line). The nuclear reflectivity (circles) of the multilayer taken by time integrating the resonant flux arriving in a time window of 23–103 ns after the nuclear excitation. The three vertical lines correspond to the angular positions of (a) the critical angle for total external reflection, (b) the pure nuclear Bragg reflection, and (c) the Bragg reflection resulting from the electronic charge periodicity. Nuclear resonant time spectra were taken at each of these angles and are shown in Fig. 3.

be time filtered electronically. An rf signal from the synchrotron storage ring provides the timing reference.

The $0.3 \text{ mm} \times 10 \text{ mm}$ beam impinging on the multilayer at low incidence angles ($<17 \text{ mrad}$) results in scattering from a significant portion of the surface. The multilayer accepts the full cross section of the beam at incidence angles $>4.2 \text{ mrad}$. The electronic, i.e., nonresonant, reflectivity of the multilayer is shown in Fig. 2. The solid line is a fit to the data using a standard optical formalism. In addition, the interface roughness was assumed to be Gaussian of width σ and was treated using the Nevót-Croce formalism [14]. The best fit required an interface roughness of $\sigma = 4 \text{ \AA}$ and a surface roughness of $\sigma = 6 \text{ \AA}$.

The time-integrated resonant signal resulted from accumulating signals arriving in a time window from 23–103 ns after the prompt radiation. The nuclear reflectivity of the multilayer, taken by measuring the time-integrated resonant signal as a function of the incident angle, is shown in Fig. 2. The peak at 3.8 mrad corresponds to coherent resonant scattering near the critical angle for total external reflection. The nuclear reflectivity grows from zero at low angles due to an increasing beam acceptance and growing penetration depth that effects an increased illumination of the ^{57}Fe nuclei. The peak has been related to the variation in the electronic reflection amplitude, being maximum where the electronic amplitude varies the strongest [15]. The peak at 16.4 mrad results from the periodicity of ^{57}Fe in the multilayer. The peak at 8.9 mrad is the pure nuclear Bragg reflection that corresponds to the periodicity enforced by the hyperfine interactions on the ^{57}Fe nuclei. The angular width of the pure nuclear Bragg peak is 1.2 mrad (FWHM). This is essentially the intrinsic angular width of the reflection due to the finite number of layers in the film because the incident radiation has an angular divergence 2 orders of magnitude less than this value. The electronic reflectivity at the angular position of the pure nuclear reflection is approximately 3×10^{-4} . As a result, the multilayer reduces the flux outside the resonant bandwidth by a factor of 3×10^{-4} , while producing a delayed, very narrow energy (5 neV) bandwidth beam. Thus, the reduced electronic reflectivity makes the multilayer a candidate for nano-eV monochromatization of synchrotron radiation.

While diffracting from the pure nuclear reflection, the time-integrated resonant counting rate was 2.5 cps. Comparison of this counting rate to that obtained with a $10 \text{ }\mu\text{m}$ thick $\alpha\text{-}^{57}\text{Fe}$ foil ($\approx 85 \text{ cps}$) demonstrated an energy-integrated nuclear reflectivity of approximately $1\Gamma_0$ ($\approx 5 \text{ neV}$). With this counting rate, the time-resolved detection of the resonantly scattered radiation produced the time spectrum shown in Fig. 3. Because of the application of the magnetic field of 0.1 T perpendicular to the scattering plane, the magnetic moments of the ^{57}Fe layers align alternately parallel and antiparallel to the scattering plane. This orientation of magnetic hyperfine

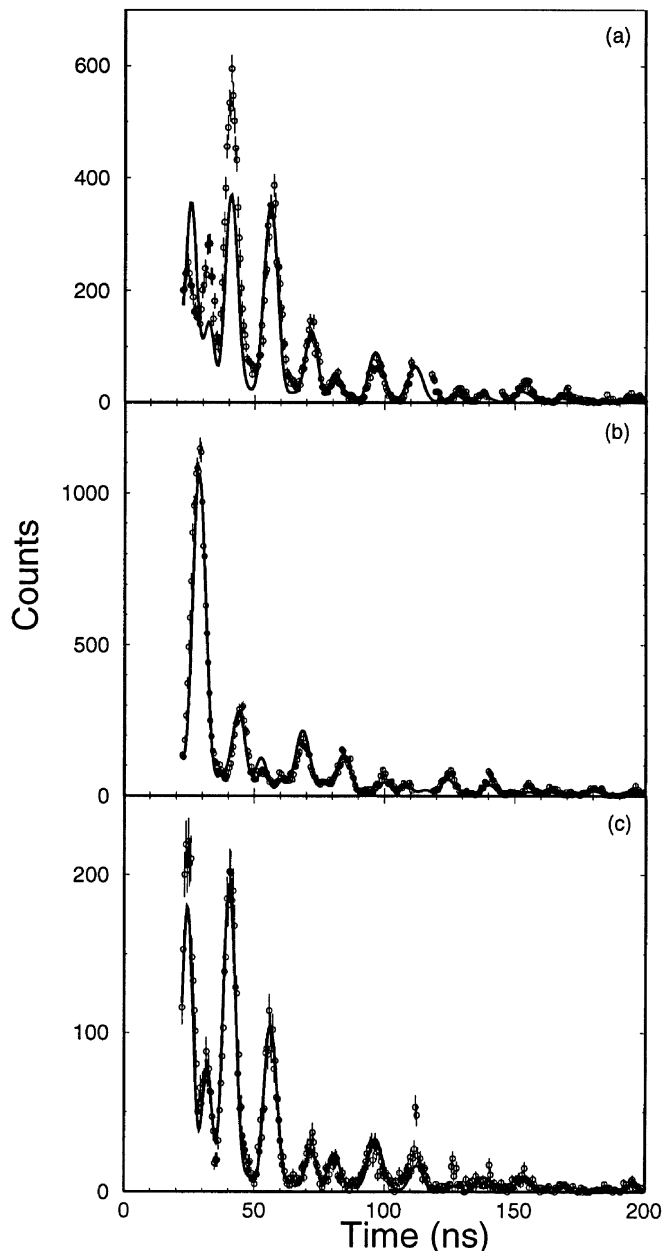


FIG. 3. Nuclear resonant time spectra taken at three different angular positions of Fig. 2. The oscillations in the time spectra result from the beating of the different frequencies associated with the different hyperfine transitions. The same model for the distribution of magnetic hyperfine fields was used to fit (solid line) all three spectra.

fields in combination with the linear polarization of the incident radiation means the resonant scattering is dominated by those transitions with $\Delta J_z = \pm 1$. These transitions correspond to lines 1, 3, 4, and 6 in the CEMS spectrum. The relationship between these resonant transitions and the beating in the time spectrum is quite similar to the case of the (111) pure nuclear reflection in $^{57}\text{FeBO}_3$ [5] without the additional component of an

electric quadrupole interaction. Time spectra taken while diffracting from both the peak near the critical angle for total external reflection and the peak corresponding to the electronically allowed Bragg reflection are also shown in Fig. 3 for comparison.

The fits are calculated based upon the theory of nuclear resonant dynamical diffraction [16] and a model for the distribution of magnetic hyperfine fields within each Fe layer. A 17 Å layer is divided into five sublayers with their thicknesses and distribution of magnetic hyperfine fields chosen to be consistent with the CEMS result. Most of the variation in the hyperfine field is assumed to be concentrated near the Fe/Cr interface. The model also assumed that the reduction of the magnetic hyperfine field at an Fe site within a layer was correlated with its proximity to the Cr layer. As a result, the sublayers possess fields that decrease in value as one approaches the Fe/Cr interface. The central region of the Fe layer (11 Å) was given the field distribution at 33.3 T. The two neighboring sublayers (2 Å) had the field distribution at 30.7 T. The next neighboring sublayers (1 Å) had the remaining field distributions as determined from the CEMS result. The resulting Fe layer possessed six different hyperfine field distributions segregated into a 1 Å–2 Å–11 Å–2 Å–1 Å structure. The fitting was complicated by the fact that the nonuniform isotopic density developed during the fabrication process. The fits are clearly not optimal but represent the sensitivity of the time spectra to the field distributions with the superlattice. Fitting all time spectra taken at different scattering angles with the same parameters to describe the multilayer exposes details of the magnetic field distributions that are difficult to see in any other way. In addition, this places an enormous constraint on any model for the magnetic field distributions that might be assumed within the Fe layers. As a result, this technique has immense potential for studying magnetic thin films containing a Mössbauer isotope.

Magnetic ordering in a synthetic multilayer has been observed with the use of nuclear resonant diffraction. The synthetic multilayer consisted of 17 Å ⁵⁷Fe layers separated by 10 Å Cr layers. Because of antiferromagnetic coupling of the ⁵⁷Fe layers that results from this Cr interlayer, the magnetic unit cell is twice the charge unit cell. These different unit cells give rise to a pure nuclear reflection. Because of the strong suppression of the electronic scattering, the pure nuclear reflection may be used for nano-eV monochromatization of synchrotron radiation in the hard x-ray regime. In addition, performing time-resolved nuclear resonant diffraction on the multilayer produces time spectra that are sensitive to the location of hyperfine fields in the layers. As a result, the technique

may be used to study thin film magnetic structures. In the future, the use of undulators will allow polarization-sensitive studies in concert with nuclear resonant diffraction to increase the ability to probe crystalline and thin film structures containing a Mössbauer isotope.

We would like to thank C. Bresloff for her assistance in the characterization of the ⁵⁷Fe/Cr film. This work is supported by US-DOE, BES Materials Science, under Contract No. W-31-109-ENG-38. The measurements at CHESS are supported by the NSF under Grant No. 90-21700.

-
- [1] P. Grünberg, R. Schreiber, Y. Pang, M. B. Brodsky, and C. H. Showers, *Phys. Rev. Lett.* **57**, 2442 (1986).
 - [2] S. S. P. Parkin, N. More, and K. P. Roche, *Phys. Rev. Lett.* **64**, 2304 (1990).
 - [3] M. N. Baibich, J. M. Broto, A. Fert, F. Nguyen Van Dau, F. Petroff, P. Eitenne, G. Creuzet, A. Friederich, and J. Chazelas, *Phys. Rev. Lett.* **61**, 2472 (1988).
 - [4] R. W. Wang, D. L. Mills, E. E. Fullerton, J. E. Mattson, and S. D. Bader, *Phys. Rev. Lett.* **72**, 920 (1994).
 - [5] U. van Bürck, R. L. Mössbauer, E. Gerdau, R. Rüffer, R. Hollatz, G. V. Smirnov, and J. P. Hannon, *Phys. Rev. Lett.* **59**, 355 (1987).
 - [6] G. Faigel, D. P. Siddons, J. B. Hastings, P. E. Hausteijn, J. R. Grover, and L. E. Berman, *Phys. Rev. Lett.* **61**, 2794 (1988).
 - [7] G. V. Smirnov, V. V. Mostovoi, Yu. V. Shvyd'ko, V. N. Seleznev, and V. V. Rudenko, *Sov. Phys. JETP* **51**, 603 (1980).
 - [8] G. V. Smirnov, V. V. Sklyarevskii, R. A. Voskanyan, and A. N. Artem'ev, *JETP Lett.* **9**, 70 (1969).
 - [9] W. Sturhahn and E. Gerdau, *Phys. Rev. B* **49**, 9285 (1994).
 - [10] A. I. Chumakov, G. V. Smirnov, A. Q. R. Baron, J. Arthur, D. E. Brown, S. L. Ruby, G. S. Brown, and N. N. Salashchenko, *Phys. Rev. Lett.* **71**, 2489 (1993).
 - [11] E. E. Fullerton, J. Pearson, C. H. Sowers, S. D. Bader, X. Z. Wu, and S. K. Sinha, *Phys. Rev. B* **48**, 17432 (1993).
 - [12] J. Landes, Ch. Sauer, R. A. Brand, W. Zinn, and Zs. Kajcsos, *Hyperfine Interact.* **57**, 1941 (1990).
 - [13] T. S. Toellner, T. Mooney, S. Shastri, and E. Alp, in *Optics for High-Brightness Synchrotron Radiation Beamlines*, edited by J. Arthur, SPIE Proceedings Vol. 1740 (SPIE—International Society for Optical Engineering, Bellingham, WA, 1993), p. 218.
 - [14] L. Nevót and C. Croce, *Rev. Phys. Appl.* **15**, 761 (1980).
 - [15] A. Q. R. Baron, J. Arthur, S. L. Ruby, A. I. Chumakov, G. V. Smirnov, and G. S. Brown, *Phys. Rev. B* (to be published).
 - [16] J. P. Hannon, G. T. Trammel, N. V. Hung, M. Mueller, E. Gerdau, R. Rüffer, and H. Winkler, *Phys. Rev. B* **32**, 5068 (1985); **32**, 6363 (1985).